J. King Saud Univ., Vol. 16, *Eng. Sci.* (2), pp. 179-202, Riyadh (1424H/2004)

Ethylene Dichloride Production in External-loop Gaslift Reactors

M.E.E. Abashar
Chemical Engineering Department, College of Engineering, King Saud University, P.O. Box 800, Riyadh 11421, Saudi Arabia
E-mail address: mabashar@ksu.edu.sa

(Received 12/6/2002; accepted for publication 29/10/2002)

Abstract. An experimental and simulation study has been carried out for the boiling temperature chlorination process of ethylene-to-ethylene dichloride in a gaslift reactor. A substantial improvement in the reactor performance is observed when perforated plate spargers are used compared to nozzle spargers. The backflow cell model is validated with experimental data and is observed to correctly predict the reactor performance in the range of experimental conditions investigated. The model has been utilized to investigate the effects of some important design (height to diameter ratio) and operating (feed ratio, top pressure) parameters on the performance of the reactor. The results suggest that tall systems with excess ethylene favor the conversion of chlorine.

Keywords: Gaslift reactors, ethylene dichloride, chlorination, backflow cell model

Notation

a_1 , a_2 gas liquid interfacial area for chlorine and ethylene bubbles respectively, m^{-1}
C_i concentration of component i in bulk liquid, mol m^{-3}
C_i^* equilibrium concentration of component i, mol m^{-3}
C_{PL} liquid heat capacity, J kg^{-1} K^{-1}
d_b bubble mean diameter, m
D_i diffusivity of component i, m^2 s^{-1}
D_L liquid phase diffusivity, m^2 s^{-1}
D_T column diameter, m
E_F enthalpy of feed gas, J m^{-2} s^{-1}

E_h axial dispersion coefficient, $m^2\ s^{-1}$

f fraction of ethylene entering liquid phase which reaches the main body of the solution without reacting chemically

F_i feed rate of component i, mol $m^{-2}\ s^{-1}$

FR feed ratio

g gravitational constant, m s^{-2}

h axial coordinate, m

HDR height to diameter ratio.

(ΔH_{Cl_2}) heat of chlorine dissolution, J mol^{-1}

(ΔH_R) heat of reaction, J mol^{-1}

(ΔH_V) heat of vaporization of ethylene dichloride, J mol^{-1}

j cell number

k_G gas phase mass transfer coefficient, mol $m^{-2}\ s^{-1}\ Pa^{-1}$

k_L^* liquid phase mass transfer coefficient, m s^{-1}

k_R reaction rate constant, $m^3\ mol^{-1}\ s^{-1}$

n total number of cells

P_i partial pressure of component i, Pa

P_i^* equilibrium vapor pressure of component i, Pa

P_T top pressure, kPa

R column radius, m

T temperature, K

U^G superficial gas velocity, m s^{-1}

U_i^G superficial flow rate of component i, mol $m^{-2}\ s^{-1}$

U^L superficial liquid velocity, m s^{-1}

V_s gas liquid slip velocity, m s^{-1}

Greek symbols

α ratio of backflow based on U^L

β reaction factor

β_∞ dimensionless parameter

γ dimensionless parameter

ε gas hold-up

η dimensionless parameter

ν_t turbulent kinematic viscosity, $m^2\ s^{-1}$

ν_L 1iquid kinematic viscosity, $m^2\ s^{-1}$

ρ_G gas density, kg m^{-3}

ρ_L liquid density, kg m^{-3}

σ_L liquid surface tension, N m^{-1}

Introduction

Gas-liquid systems with and without chemical reactions are of great importance in the chemical and biochemical industries [1,2]. The potential application of gaslift reactors to gas-liquid systems has gained increasing attention, and this field promises to be even more fertile. This is because the gaslift reactors are efficient gas-liquid contactors and characterized by low cost, high mass and heat transfer coefficients, high capacity, good mixing and absence of mechanical agitators [3]. However, models describing the gaslift reactors, especially when mass transfer accompanied chemical reactions, are limited [4]. The main difficulty in the mathematical modeling and design of gaslift reactors has been the lack of information on the hydrodynamics [5].

A comprehensive picture of problems that are encountered in the filed of mass transfer with chemical reaction in gas-liquid systems is presented by Doraiswamy and Sharma [6]. Production of ethylene dichloride is an example of a gas-liquid system in which chemical reaction is coupled with mass transfer and heat transfer. Ethylene dichloride (EDC), also known as 1,2-dichloroethane, is used to produce vinyl chloride monomer (VCM), which is involved in production of polyvinyl chloride (PVC). Ethylene dichloride can also be used as a solvent and in the manufacture of other organic compounds.

Ethylene dichloride can be produced industrially at low temperature of 40-60 ^oC by conventional chlorination methods [7,8]. The gas-liquid heterogeneous reaction of ethylene and chlorine is carried out: (a) in a body of ethylene dichloride in a well-mixed stirred tank reactor and, (b) in a packed or empty reactor with a circulating stream of ethylene dichloride. Wachi and Morikawa [9] have reported that the gaslift reactors with external loops are efficient contactors for production of ethylene dichloride by a boiling temperature (80-140 ^oC) addition chlorination process. The chlorination process of this type offers advantages over conventional chlorination processes from the standpoint of energy saving and product (ethylene dichloride) separation. The authors have also shown that at their experimental conditions the behavior of the reactor is well predicted by the backflow cell model. However, their results suggest that more investigations are needed to evaluate the effect of different hydrodynamic parameters on the reliability of the backflow cell model.

Gaslift reactors have many hydrodynamic variables [1]. These variables are classified as independent variables such as superficial gas velocity (independently controllable), the physical properties of the fluids and reactor geometry. Some of the other dependent variables are gas hold-up, liquid circulation velocity, bubble characteristics (size, velocity, coalescence, frequency, etc.), heat transfer, mass transfer

and dispersion coefficients. All these variables are strongly interrelated in the fabric of gaslift reactors. In fact, the geometry of the reactor has a strong influence on the hydrodynamics and this factor is a source of difficulty in comparing different results. In particular, the sparger parameters can, at times, greatly influence the reactor behavior.

In spite of the availability of various conventional methods for production of ethylene dichloride, systematic knowledge on the hydrodynamic characteristics of the boiling temperature addition chlorination process is lacking in the literature. The aim of this work is to examine the influence of the sparger parameters on the production of ethylene dichloride by the boiling temperature addition chlorination process. Two types of spargers are considered. Furthermore, the reliability of the backflow cell model is evaluated. The model is also tested for its sensitivity to changes in hydrodynamic parameters. Hopefully by continual evaluation of the efficiency of our tools and methods, unified models applicable to all gaslift reactors in all their variety can be developed for this industrially important chlorination process.

Experimental

A schematic diagram of the pilot plant, external-loop gaslift reactor used in this study for the boiling addition chlorination process is shown in Fig. 1. The reactor was made of borosilicate glass and composed of riser and downcomer with inside diameters of 0.14 m and dispersion heights of 5.8 m and a gas separator (length: 2.0 m, height: 0.8 m, width: 0.3 m). Two spargers are used: a single orifice nozzle (5 mm in diameter) and a circular perforated plate (50 holes of 1 mm uniformly spaced). A separate sparger for each gas was used. Concentration, temperature and pressure were taken at seven locations in the riser. The reactor was first filled with ethylene dichloride liquid. Then, ethylene and chlorine were separately introduced at constant feed rate and temperature through the spargers. The flow rates of the gaseous ethylene and chlorine were measured by turbine flowmeters and controlled by needle valves just downstream of them. The liquid circulation in the downcomer was measured by an ultrasonic Doppler flowmeter and controlled by a butterfly valve located at the bottom section. Part of the ethylene dichloride formed was recycled to keep the volume of the liquid constant. The pressure at the top of the reactor was kept constant by control of gas ventilation from the gas separator. To suppress the side reactions, a small amount of ferric chloride and oxygen were added as catalysts. The ferric chloride was added to the liquid phase and the oxygen was fed continuously with gaseous chlorine. The reactor was well insulated for adiabatic conditions. Iodine titration was used to determine the dissolved chlorine concentration and a gas chromatograph was used to analyze the unreacted gas at the top of the reactor.

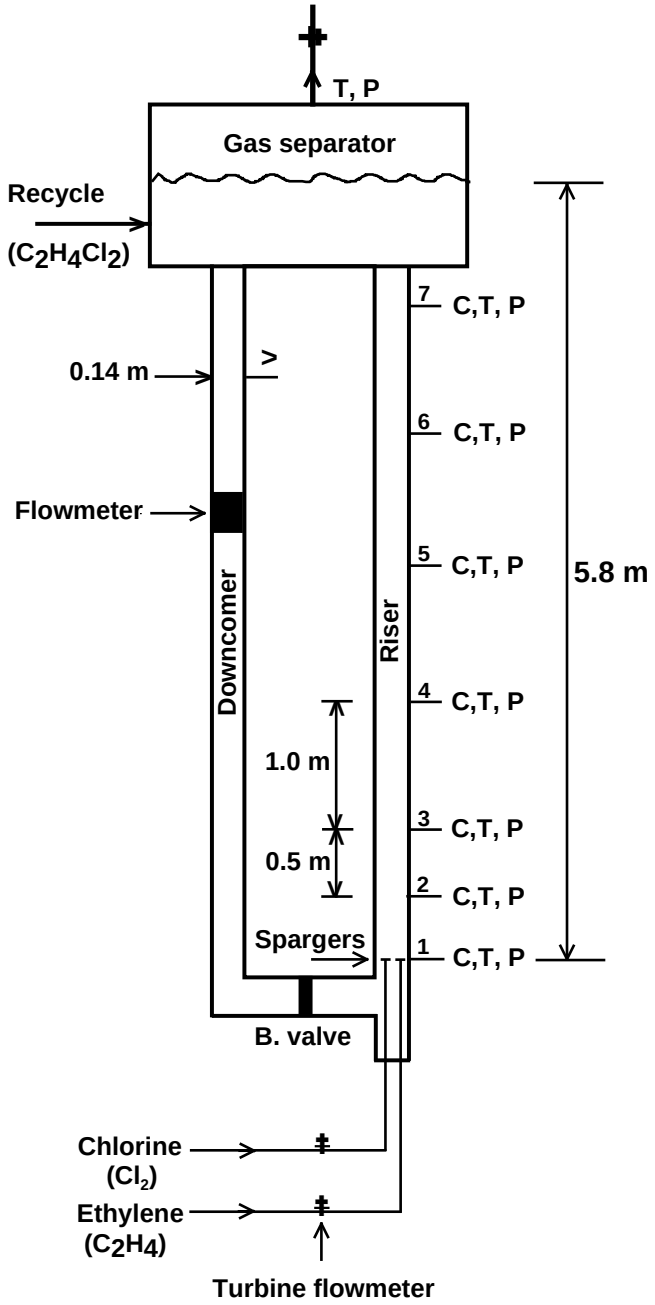

Fig. 1. Schematic diagram of the external-loop gaslift reactor.

Model Development

The problem investigated is that of the exothermic gas-liquid heterogeneous reaction for the formation of ethylene dichloride by simultaneous absorption and reaction of ethylene and chlorine in boiling ethylene dichloride liquid.

$$C_2H_4 + Cl_2 \rightarrow C_2H_4Cl_2 \quad (1)$$

A backflow cell model (BFCM) is developed for the cocurrent two-phase gaslift reactor [9-11]. The backflow cell model describes axial mixing effects by a detailed analysis of back flows between the cells with greater rigor than a differentially continuous diffusion model with a constant axial dispersion coefficient for the liquid phase. A schematic representation of the model is shown in Fig. 2. The following assumptions are made:

1. Adiabatic and steady state conditions.
2. Mixing between chlorine and ethylene bubbles is negligible.
3. Liquid volume is kept constant.
4. Chlorine and ethylene dissolve separately in the ethylene chloride and reaction occurs in the liquid phase [7].
5. The reaction is assumed to take place close to the surface of the ethylene bubble. This assumption is justified by the fact that the solubility of chlorine is about seven times that of ethylene and their diffusivities are about equal [7].
6. The liquid phase mass transfer resistance controls the absorption rate of ethylene and chlorine [9].
7. The cell is perfectly mixed.
8. Vaporization of ethylene dichloride is controlled by the gas phase resistance of mass transfer [9].
9. Henry's law applies [11].
10. The pressure and the gas hold-up depend on height, h [11].
11. Heat transfer by conduction is negligible [9].

(a) Mass Balance

The equations related to mass balance for the gas and liquid phases are given below based on the description in Fig. 3.

(i) Gas phase

Mass balances on chlorine, ethylene and ethylene dichloride in the gas phase of the j-th cell gives the following equations

$$F_{Cl_2}(j) + U^G_{Cl_2}(j-1) = U^G_{Cl_2}(j) + k^*_L a_1 \left[C^*_{Cl_2} - C_{Cl_2}(j) \right] \Delta h \quad (2)$$

$$F_{C_2H_4}(j)+U^G_{C_2H_4}(j-1)=U^G_{C_2H_4}(j)+\beta k_L^* a_2\left[C^*_{C_2H_4}-C_{C_2H_4}(j)\right]\Delta h \tag{3}$$

$$U^G_{EDC,m}(j-1)+k_G\, a_m(P^*_{EDC}-P_{EDC,m})\,\Delta h=U^G_{EDC,m}(j) \tag{4}$$

where $m=1,2$ for chlorine and ethylene bubbles respectively. The terms $F_i(j), T_F(j)$ and $E_F(j)$ appear only at the feed cell.

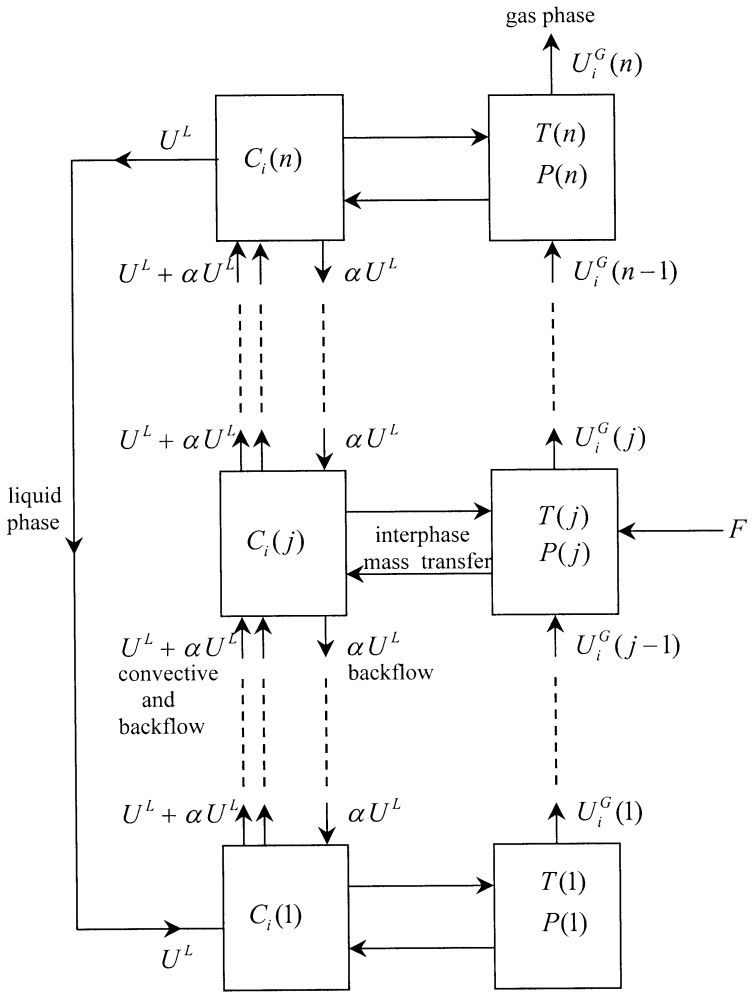

Fig. 2. Schematic representation of BFCM for cocurrent flow.

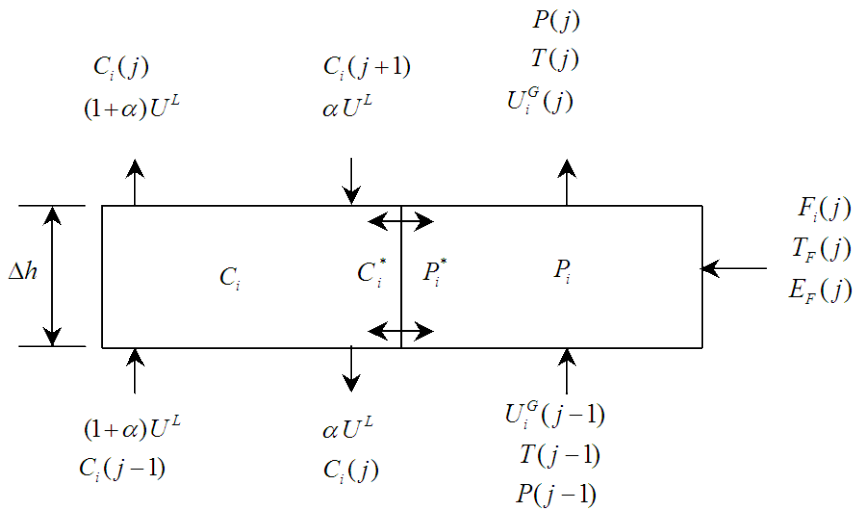

Fig. 3. Schematic representaiton of the j-th backflow cell.

(ii) Liquid phase

A mass balance on chlorine in the liquid phase of the first, j-th and n-th cells gives the following equations

$$\begin{aligned} &U^L C_{Cl_2}(n) + \alpha U^L C_{Cl_2}(2) + k_L^*\, a_1\left[C_{Cl_2}^* - C_{Cl_2}(1)\right]\Delta h = \\ &(1+\alpha)U^L C_{Cl_2}(1) + (1-\varepsilon(j))\,k_R C_{Cl_2}(1)\,C_{C_2H_4}(1)\Delta h \\ &+ (1-f)\,\beta k_L^*\, a_2\left[C_{C_2H_4}^* - C_{C_2H_4}(1)\right]\Delta h \end{aligned} \tag{5}$$

$$\begin{aligned} &(1+\alpha)U^L C_{Cl_2}(j-1) + \alpha U^L C_{Cl_2}(j+1) + k_L^*\, a_1\left[C_{Cl_2}^* - C_{Cl_2}(j)\right]\Delta h = \\ &(1+2\alpha)U^L C_{Cl_2}(j) + (1-\varepsilon(j))\,k_R C_{Cl_2}(j)\,C_{C_2H_4}(j)\Delta h \\ &+ (1-f)\,\beta k_L^*\, a_2\left[C_{C_2H_4}^* - C_{C_2H_4}(j)\right]\Delta h \end{aligned} \tag{6}$$

$$\begin{aligned} &(1+\alpha)U^L C_{Cl_2}(n-1) + k_L^*\, a_1\left[C_{Cl_2}^* - C_{Cl_2}(n)\right]\Delta h = \\ &(1+\alpha)U^L C_{Cl_2}(n) + (1-\varepsilon(j))\,k_R C_{Cl_2}(n)\,C_{C_2H_4}(n)\Delta h \\ &+ (1-f)\,\beta k_L^*\, a_2\left[C_{C_2H_4}^* - C_{C_2H_4}(n)\right]\Delta h \end{aligned} \tag{7}$$

A mass balance on ethylene in the liquid phase of the first, j-th and n-th cells gives the following equations

$$U^L C_{C_2H_4}(n) + \alpha U^L C_{C_2H_4}(2) + \beta k_L^* a_2 \left[C^*_{C_2H_4} - C_{C_2H_4}(1) \right] \Delta h =$$
$$(1+\alpha) U^L C_{C_2H_4}(1) + (1-\varepsilon(j)) k_R C_{Cl_2}(1) C_{C_2H_4}(1) \Delta h$$
$$+ (1-f) \beta k_L^* a_2 \left[C^*_{C_2H_4} - C_{C_2H_4}(1) \right] \Delta h \quad (8)$$

$$(1+\alpha) U^L C_{C_2H_4}(j-1) + \alpha U^L C_{C_2H_4}(j+1) + \beta k_L^* a_2 \left[C^*_{C_2H_4} - C_{C_2H_4}(j) \right] \Delta h =$$
$$(1+2\alpha) U^L C_{C_2H_4}(j) + (1-\varepsilon(j)) k_R C_{Cl_2}(j) C_{C_2H_4}(j) \Delta h$$
$$+ (1-f) \beta k_L^* a_2 \left[C^*_{C_2H_4} - C_{C_2H_4}(j) \right] \Delta h \quad (9)$$

(9)

$$(1+\alpha) U^L C_{C_2H_4}(n-1) + \beta k_L^* a_2 \left[C^*_{C_2H_4} - C_{C_2H_4}(n) \right] \Delta h =$$
$$(1+\alpha) U^L C_{C_2H_4}(n) + (1-\varepsilon(j)) k_R C_{Cl_2}(n) C_{C_2H_4}(n) \Delta h$$
$$+ (1-f) \beta k_L^* a_2 \left[C^*_{C_2H_4} - C_{C_2H_4}(n) \right] \Delta h \quad (10)$$

where the liquid-side mass transfer coefficient is given by [12]

$$\frac{k_L^* d_b}{D_L} = 0.5 \left(\frac{\nu_L}{D_L} \right)^{1/2} \left(\frac{g d_b^3}{\nu_L^2} \right)^{1/4} \left(\frac{g d_b^2 \rho_L}{\sigma_L} \right)^{3/8} \quad (11)$$

and the gas liquid interfacial area is given by

$$a_m = \frac{6\varepsilon}{d_{b,m}} \qquad , \qquad m = 1, 2 \quad (12)$$

The gas hold-up is given by [13]

$$\varepsilon = \frac{-(U^L + U^G + V_s) \sqrt{(U^L + U^G + V_s)^2 + 4U^G \left(\frac{gR^2}{48\nu_t} - V_s \right)}}{2 \left(\frac{gR^2}{48\nu_t} - V_s \right)} \left[1 - \exp\left(\frac{-h}{0.4U^L} \right) \right] \quad (13)$$

where

$$\nu_t = 0.128 D_T^{1.7} \quad (14)$$

and the gas liquid slip velocity is given by [1]

$$V_s = 1.53 \left[\frac{\sigma_L g (\rho_L - \rho_G)}{\rho_L^2} \right]^{0.25} \quad (15)$$

The backflow ratio is given by [10]

$$\alpha = \frac{E_h}{U^L \Delta h} - \frac{1}{2} \tag{16}$$

and the axial dispersion coefficient is given by [9]

$$E_h = \frac{(1-\varepsilon)R^2}{8\nu_t}\left[\begin{array}{l}\frac{11}{96}\left(\frac{\tau_w R}{\rho_L \nu_t}\right)^2 + \frac{73}{17280}\left(\frac{g\,\varepsilon\, R^2}{\nu_t}\right)^2 + \left(V_W - \frac{U^L}{1-\varepsilon}\right)^2 \\ + \frac{7}{160}\frac{g\,\varepsilon\,\tau_w R^3}{\rho_L \nu_t^{\,2}} + \left(\frac{g\,\varepsilon\, R^2}{8\nu_t} + \frac{\tau_w R}{3\rho_L \nu_t}\right)\left(V_W - \frac{U^L}{1-\varepsilon}\right)\end{array}\right] + \frac{\nu_t}{(1-\varepsilon)} \tag{17}$$

where

$$\tau_w = \frac{\rho_L V_w^2}{(11.63)^2} \tag{18}$$

$$V_W = \frac{U^L}{(1-\varepsilon)} - \left(\frac{\tau_W R}{12\,\rho_L \nu_t}\right)\left(\frac{3-4\varepsilon}{1-\varepsilon}\right) - \left(\frac{gR^2\varepsilon}{48\nu_t}\right)\left(\frac{2-3\varepsilon}{1-\varepsilon}\right) \tag{19}$$

The chemical reaction rate constant is given by [9]

$$k_R = 5.36\times 10^2 \exp\left(\frac{-2518.0}{T}\right) \tag{20}$$

The fraction of ethylene which diffuses into the main body of the liquid without reacting chemically is

$$f = \frac{C_{C_2H_4}\cosh(\eta\gamma) - C^*_{C_2H_4}}{C^*_{C_2H_4} - C_{C_2H_4}\cosh(\eta\gamma)} \tag{21}$$

The reaction (enhancement) factor is given by [12]

$$\beta = \left[\eta\gamma + \left(\frac{\pi}{8\eta\gamma}\right)\right] erfc\left(\frac{2\eta\gamma}{\sqrt{\pi}}\right) + \frac{1}{2}\exp\left(-\frac{4(\eta\gamma)^2}{\pi}\right) \tag{22}$$

where

$$\gamma = \frac{\sqrt{k_R C_{Cl_2} D_{C_2H_4}}}{k_L^*} \tag{23}$$

$$\eta = \sqrt{\frac{C_{Cl_2}^*}{C_{Cl_2}}} = \sqrt{\frac{(\beta_\infty - \beta)}{(\beta_\infty - 1)}} \tag{24}$$

$$\beta_\infty = 1 + \frac{C_{Cl_2}}{C_{C_2H_4}^*}\sqrt{\frac{D_{Cl_2}}{D_{C_2H_4}}} \tag{25}$$

The vapor pressure of ethylene dichloride is given by Antoine equation [14]

$$\ln P_{EDC}^* = 14.3572 - \frac{3069.08}{T - 42.3468} \tag{26}$$

(b) Energy balance

The energy balance equations for the first, j-th and n-th cells are given by

$$\begin{aligned} &E_F(1) + U^L \rho_L C_{PL} T(n) + \alpha U^L \rho_L C_{PL} T(2) \\ &+(\Delta H_R)\begin{bmatrix}(1-\varepsilon(j))\, k_R C_{Cl_2}(1) C_{C_2H_4}(1) \; + \\ (1-f)\,\beta\, k_L^*\, a_2 \left(C_{C_2H_4}^* - C_{C_2H_4}(1)\right)\end{bmatrix}\Delta h \\ &+(\Delta H_{Cl_2})\, k_L^*\, a_1 \left(C_{Cl_2}^* - C_{Cl_2}(1)\right)\Delta h = \\ &(1+\alpha) U^L \rho_L C_{PL} T(1) + (\Delta H_V)\left[\sum_{m=1}^{2} k_G a_m (P_{EDC}^* - P_{EDC,m})\right]\Delta h \end{aligned} \tag{27}$$

$$\begin{aligned} &E_F(j) + (1+\alpha) U^L \rho_L C_{PL} T(j-1) + \alpha U^L \rho_L C_{PL} T(j+1) \\ &+(\Delta H_R)\begin{bmatrix}(1-\varepsilon(j))\, k_R C_{Cl_2}(j) C_{C_2H_4}(j) \; + \\ (1-f)\,\beta\, k_L^*\, a_2 \left(C_{C_2H_4}^* - C_{C_2H_4}(j)\right)\end{bmatrix}\Delta h \\ &+(\Delta H_{Cl_2})\, k_L^*\, a_1 \left(C_{Cl_2}^* - C_{Cl_2}(j)\right)\Delta h = \\ &(1+2\alpha) U^L \rho_L C_{PL} T(j) + (\Delta H_V)\left[\sum_{m=1}^{2} k_G a_m (P_{EDC}^* - P_{EDC,m})\right]\Delta h \end{aligned} \tag{28}$$

$$
\begin{aligned}
&E_F(n)+(1+\alpha)U^L\rho_L C_{PL}T(n-1)\\
&+(\Delta H_R)\begin{bmatrix}(1-\varepsilon(j))k_R C_{Cl_2}(n)C_{C_2H_4}(n)\ +\\ (1-f)\beta k_L^* a_2\left(C^*_{C_2H_4}-C_{C_2H_4}(n)\right)\end{bmatrix}\Delta h\\
&+(\Delta H_{Cl_2})k_L^* a_1\left(C^*_{Cl_2}-C_{Cl_2}(n)\right)\Delta h=\\
&(1+\alpha)U^L\rho_L C_{PL}T(n)+(\Delta H_V)\left[\sum_{m=1}^{2}k_G a_m(P^*_{EDC}-P_{EDC,m})\right]\Delta h
\end{aligned}
\tag{29}
$$

(c) Momentum balance

The pressure balance for j-th cell gives

$$P(j)=P(j+1)+\rho_L\, g\left[1-\frac{\varepsilon(j)+\varepsilon(j+1)}{2}\right]\Delta h \tag{30}$$

Computational Algorithm

As the mass, energy and momentum balance equations (2-10,27-30) are nonlinear algebraic equations an iterative solution was used. The equations were numerically solved by successive overrelaxation method (SOR). This iterative method takes advantage of the fact that the matrix of the coefficients consists mainly of zeros. So linearization of the equations is not needed. Double precision was used to ensure the accuracy of the solution. The convergence was obtained by a cell number of 60 ($n=60$). For $n>60$, the conversion becomes insensitive to number of cells.

Results and Discussion

We now consider and compare the performance of the reactor using perforated plate and nozzle spargers under the same conditions. We also evaluate the model predictions with the experimental data.

The reactant gases (C_2H_4, Cl_2) are fed separately through the same type of spargers to the reactor at the same flow rate of 30 Nm^3/h i.e. the feed ratio (FR) is kept constant at unity. The top pressure and the temperature are maintained at 245 kP and 115.75 ^oC respectively.

Figure 4 shows a comparison between experimental values of temperature along the riser and those calculated from the backflow cell model for various superficial liquid velocities in the reactor with perforated plate spargers. The temperature at the top of the reactor is kept at the boiling temperature of ethylene dichloride (T=115.75 ^oC). It can be observed that the agreement between the model and experiments is satisfactory except at the region close to the gas spargers. The general trend observed in this region is that the temperature profiles pass through minima as well as maxima. The decrease and the steep initial rise in the temperature could be due to the balance between the heat of

reaction and heat of vaporization of ethylene dichloride. Beyond this region the temperature tends to homogenize along the riser by the strong influence of axial dispersion on convective heat transfer. It can be seen, that the increase of the liquid flow reduces the peak temperature. However, the size of this complex region is increased by the increase of the superficial liquid velocity.

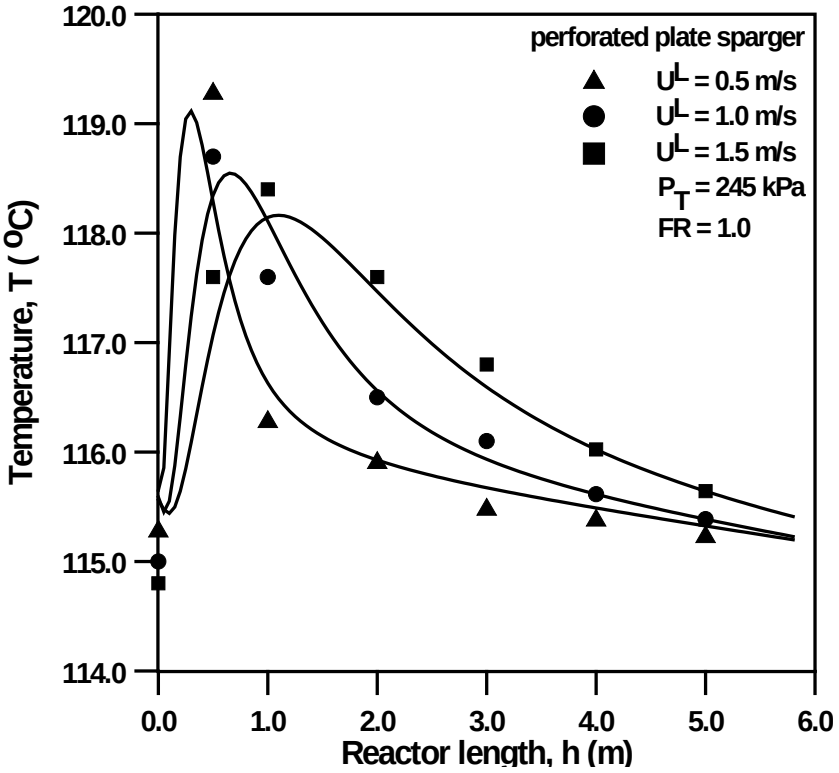

Fig. 4. Comparison of simulated (lines) and experimental (data points) results. Temperature profiles in the reactor with perforated plate spargers at various superficial liquid velocities.

For the case of the nozzle spargers, the temperature along the riser is presented in Fig. 5. Comparing the profiles in the reactor with the perforated and nozzle spargers, it becomes clear that the type of the sparger has profound influence on the reactor performance. It seems that for both cases the poor prediction of the backflow cell model to this region is caused by lack of sufficient knowledge of the complex mass and heat transfer accompanied the chlorination reaction. The perforated plate sparger has a significant advantage over the nozzle sparger by decreasing the size of this complex region i.e. the maximum distance necessary for the equilibrium bubble size. This could be due to the uniform bubbles produced by the perforated plate sparger.

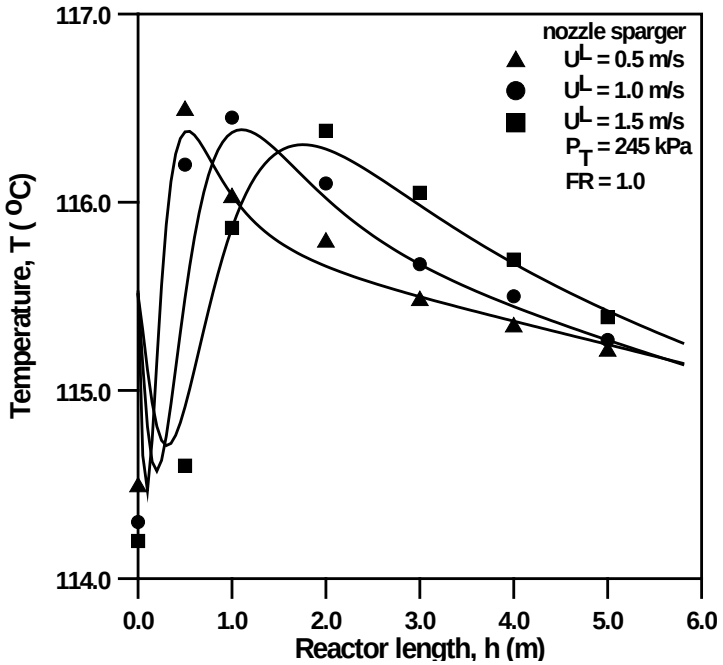

Fig. 5. Comparison of simulated (lines) and experimental (data points) results. Temperature profiles in the reactor with nozzle spargers at various superficial liquid velocities.

Figure 6 shows the predicted gas hold-up profiles in the reactor with perforated plate spargers for various superficial liquid velocities. The experimental axial distributions of the gas hold-up are also shown. The sharp increase in the gas hold-up at the bottom of the reactor (region close to the spargers) could be due to the significant vaporization of ethylene dichloride formed by the chlorination reaction. It is also shown that the increase of the liquid flow rate has significant decrease of the gas hold-up. Regarding the nozzle spargers the same trends in the reactor with the perforated plate spargers are found as shown in Fig. 7. However, higher gas hold-up values are observed in the case of the nozzle spargers. This is because the gas hold-up is enhanced by the large bubbles formed by the nozzle spargers.

Figure 8 displays the predicted axial concentration profiles of chlorine in bulk liquid in the reactor with perforated plate spargers at different superficial liquid velocities. Also shown is the experimental data. The major trend observed is an initial steep rise in the chlorine concentration at the entrance of the reactor. This rise attains a maximum and the dissolved chlorine then is rapidly consumed by the chemical reaction. It can be seen that the model correctly predicts the main trends after one meter from the

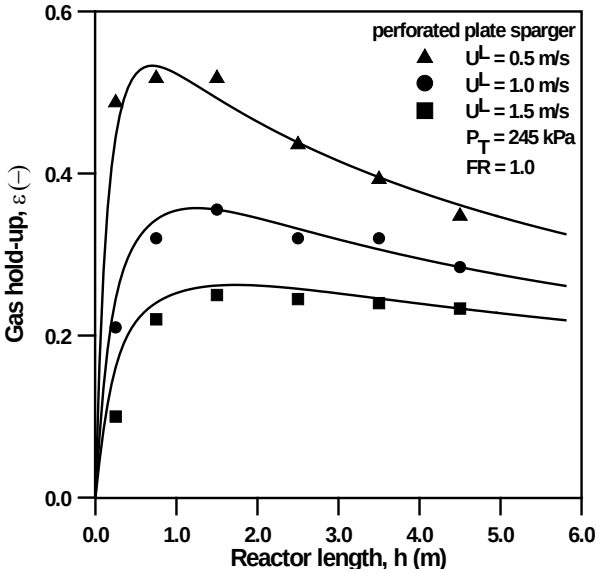

Fig. 6. Comparison of simulated (lines) and experimental (data points) results. Gas hold-up profiles in the reactor with perforated plate spargers at various superficial liquid velocities.

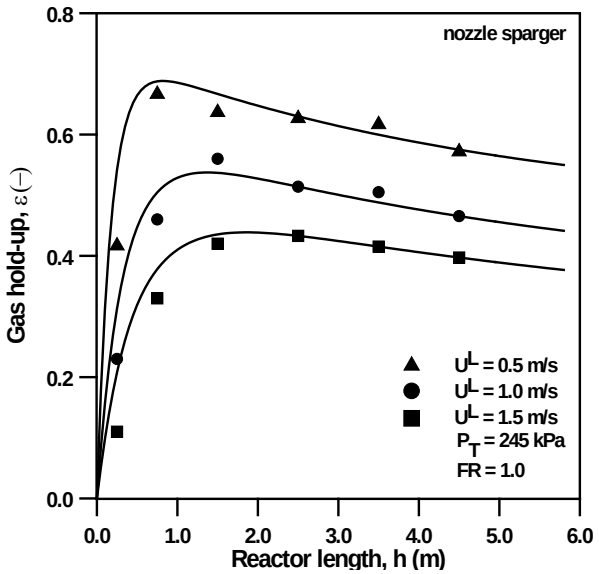

Fig. 7. Comparison of simulated (lines) and experimental (data points) results. Gas hold-up profiles in the reactor with nozzle spargers at various superficial liquid velocities.

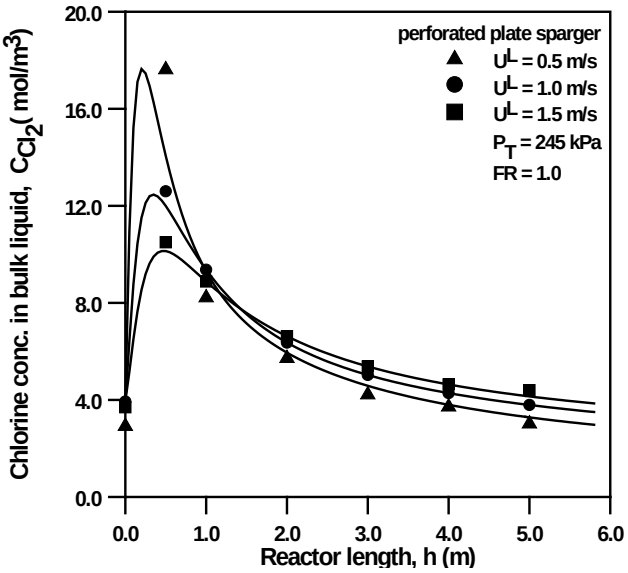

Fig. 8. Comparison of simulated (lines) and experimental (data points) results. Chlorine concentration profiles in the reactor with perforated plate spargers at various superficial liquid velocities

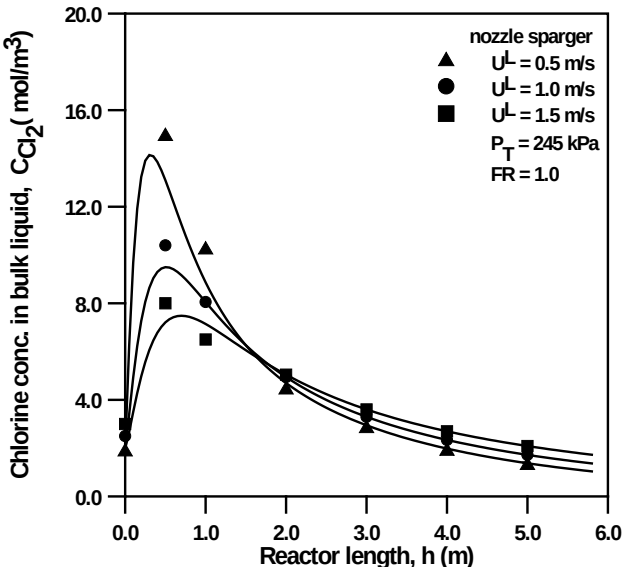

Fig. 9. Comparison of simulated (lines) and experimental (data points) results. Chlorine concentration profiles in the reactor with nozzle spargers at various superficial liquid velocities.

sparger location. It is also shown that the maxima are sensitive to the liquid flow rate. For the nozzle spargers, the chlorine concentration profiles along the riser are presented in Figure 9. It is clearly shown that for the nozzle spargers the absorption rate of chlorine is low due to the limited area for mass transfer of large bubbles. This high by-pass of chlorine is reflected by high gas hold-up in Fig. 7. The discrepancies between outcomes of the simulations and the experiments at the bottom of the reactor are clearly shown in Figure 9.

As mentioned above, the manner in which gas is distributed has an important influence on the reactor performance. It has been observed that the perforated plate sparger produces uniform bubble distribution and better reactor performance. Therefore, in the analyses that follow the reactor with perforated plate is considered for further investigations.

The simulation result of ethylene concentration in bulk liquid along the reactor for various superficial velocities is shown in Figure 10. As can be seen from Figure 8, the solubility of ethylene is much less than that of chlorine. This evidence justifies the assumption that the reaction occurs in the liquid phase and the reaction zone (or plane) is close to the surface of the ethylene bubble. It appears that under our operating conditions the liquid flow rate does not have significant effect on the solubility of ethylene.

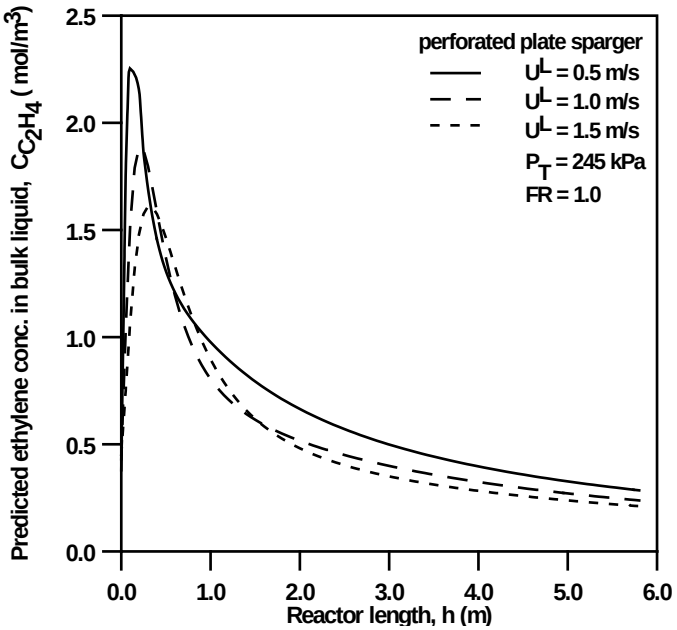

Fig. 10. Predicted ethylene concentration profiles in the reactor with perforated plate spargers at various superficial liquid velocities.

Parametric analysis

The backflow cell model is used to determine the sensitivity of several important design and operating parameters, such as the height to diameter ratio (HDR), reactants feed ratio (FR) and top pressure. This type of parametric investigation gives better insight into the performance of the reactor beyond the experiment limits imposed by economic and safety considerations.

(a) Effect of Feed Ratio (FR)

Figure 11 shows the influence of varying the reactants feed ratio (FR) on the chlorine concentration in the bulk liquid. The feed ratio of reactants, defined as the flow rate of ethylene divided by the flow rate of chlorine, is varied by changing the flow rate of ethylene and the flow rate of chlorine is maintained constant at 30 Nm^3/h. It can be seen that the excess of ethylene has a large impact on the dissolved chlorine. High feed ratio favors the conversion of chlorine and a substantial decease in the concentration is observed. Low concentration of chlorine in bulk liquid is preferable since at high concentrations of chlorine the proportion of higher chlorinated products (mainly trichloroethanes) tends to increase. Furthermore high concentrations of chlorine enhance the corrosion problems. The corresponding gas hold-up is shown in Fig. 12. As expected, the gas hold-up increased with feed ratio.

(b) Effect of Height to Diameter Ratio (HDR)

Figure 13 shows the effect of the height to diameter ratio (HDR) i.e. aspect ratio on the chlorine concentration in bulk liquid. The HDR calculations are performed by the height was held constant and the diameter was decreased. The U^L was kept constant by controlling the circulation flowrate by the butterfly valve shown in Fig. 1. As the height to diameter ratio increases, the length of the reactor increases which results in an increase in the dissolved chlorine concentration. This could be due to the increase in the mixing time and the gas hold-up as shown in Fig. 14. The results indicate that the effect of the height to diameter ratio on the gas hold-up is very prominent.

(c) Effect of top pressure

The top pressure has a strong influence on the boiling temperature of ethylene dichloride liquid. The effect of the top pressure on the temperature profiles along the reactor is presented in Figure 15. It is shown that the temperature reaches a maximum close to the bottom of the reactor and then drops and approaches asymptotically the boiling temperature of ethylene dichloride at the top of the reactor. Figure 16 shows the corresponding chlorine concentration in bulk liquid. The results indicate that although the variation of the top pressure has an effect on the temperature, there is no noticeable influence on the dissolved chlorine, which could be due to the increased rate of reaction via increase in temperature. It is interesting that the effect of the top pressure is more pronounced on the gas hold-up as shown in Fig. 17.

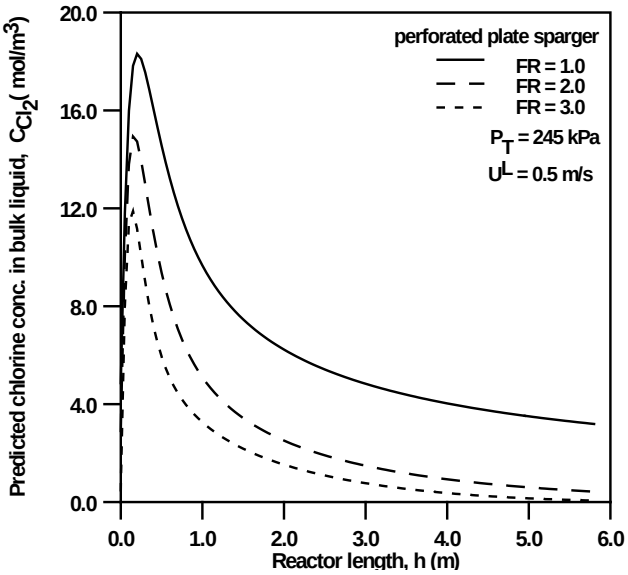

Fig. 11. Effect of feed ratio on the predicted chlorine concentration.

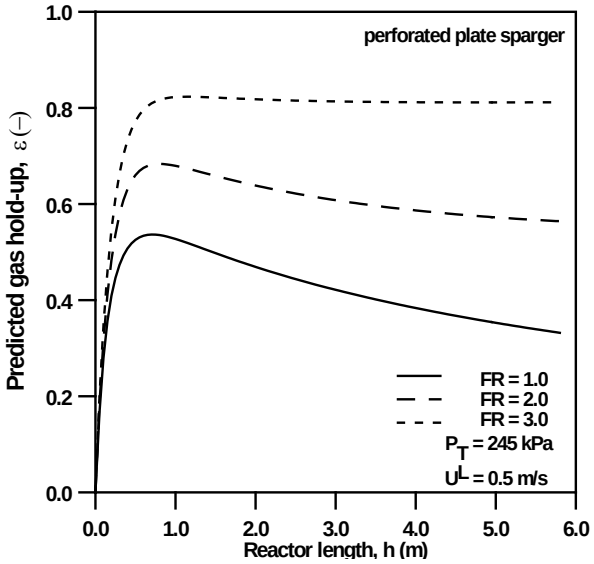

Fig. 12. Effect of feed ratio on the predicted gas hold-up.

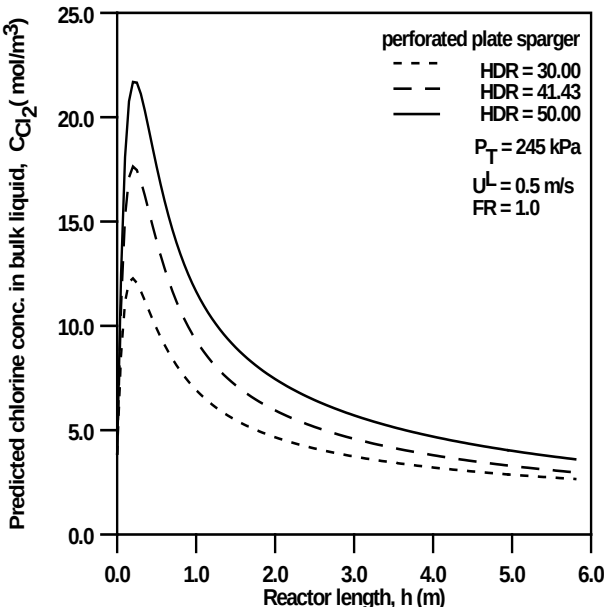

Fig. 13. Effect of height to diameter ratio on the predicted chlorine concentration.

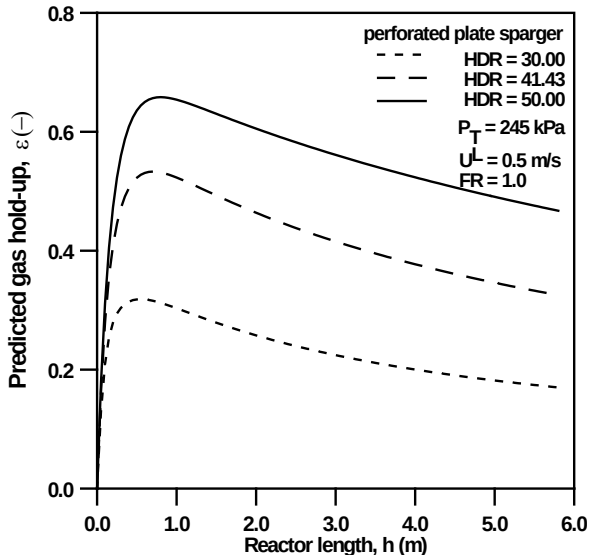

Fig. 14. Effect of height to diameter ratio on the predicted gas hold-up.

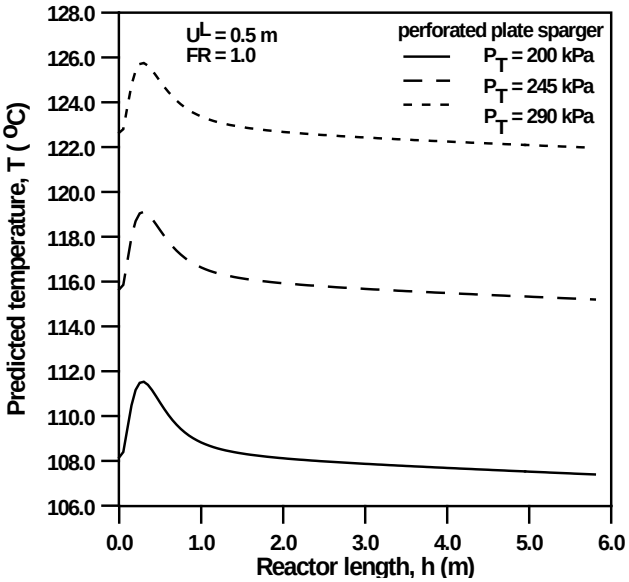

Fig. 15. Effect of top pressure on the predicted temperature.

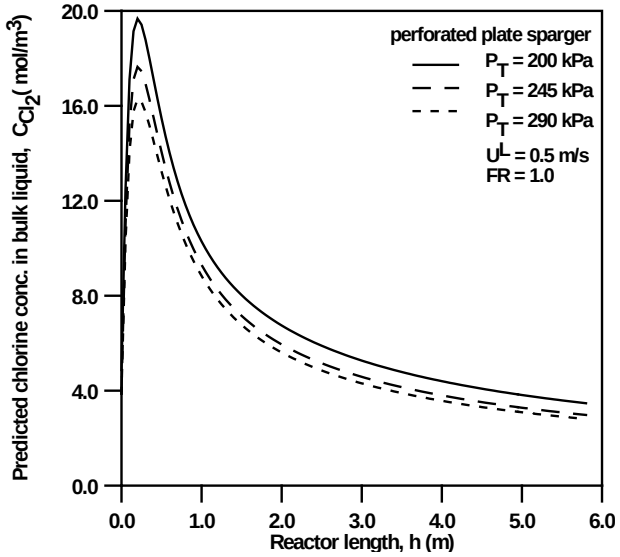

Fig. 16. Effect of top pressure on the predicted chlorine concentration.

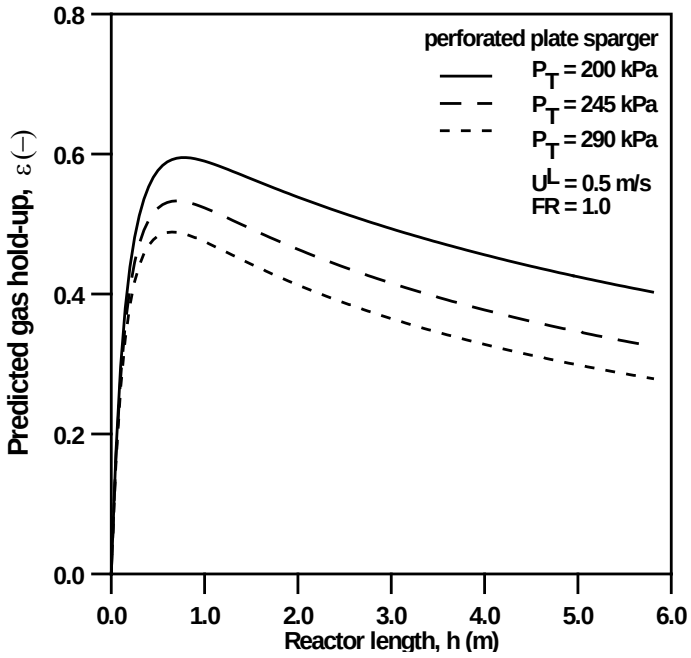

Fig. 17. Effect of top pressure on the predicted gas hold-up.

Conclusions

A backflow model has been used to investigate the behavior of a gaslift reactor with perforated plate and nozzle spargers for the production of ethylene dichloride by the boiling temperature chlorination process. Model predictions are validated by experimental measurements. Good agreement is obtained between the experimental data and those predicted by the mathematical model. Discrepancies are observed between the mathematical model and experiment results in the neighborhood of the spargers. It must be clearly recognized that this region is fairly complex and should be subjected to further theoretical and experimental investigations. As a conclusion, the proposed mathematical model is shown to be reliable and efficient.

Comparing the perforated plate sparger and nozzle sparger, we see that the reactor is much more efficient when operated with perforated plate sparger. This indicates that the initial bubble size and distribution is very important. However, this does not mean that everywhere else the perforated plate sparger is better. It is still interesting to attempt to define a means by which different spargers can be equitably compared.

The model predicts that the use of excess ethylene should facilitate the

consumption of dissolved chlorine. The simulation results also indicate that the height to diameter ratio has strong influence on the chlorine conversion i.e. tall gaslift reactors favor the conversion of chlorine. It is also predicted that varying the top pressure does not significantly change the dissolved chlorine concentration.

The work along the directions of studying the hydrodynamic characteristics of the sparger zone, gas separator and downcomer is currently in progress. More meaningful evaluation of the reactor performance will probably have to await the industrial test of the technology.

References

[1] Abashar, M. E., Narsingh,U., Rouillard, A. E. and Judd, R. "Hydrodynamic Flow Regimes, Gas Holdup, and Liquid Circulation in Airlift Reactors." *Ind. Eng. Chem. Res.*, 37 (1998) ,1251-1259.

[2] Abashar, M. E. "Influence of Hydrodynamic Flow Regimes on the Prediction of Gas Hold-up and Liquid Circulation in Airlift Reactors." *J. of King Saud Univ.* (*Eng. Sci.*), 6, No. 1 (2002), 97-111.

[3] Chisti, M. Y. *Air-lift Bioreactors*, Elsevier. New York: Applied Science, 1989.

[4] Garcia Calvo, E. G. and Leton, P. A. "Fluid Dynamic Model for Air-lift Reactors." *Chem. Eng. Sci.*, 46 (1991), 2947-2951.

[5] Merchuk, J. C. and Stein, Y. A. "Distributed Parameter Model of an Air-Lift Reactors." *AIChE J*, 27, No. 3 (1981), 377-388.

[6] Doraiswamy, L. K. and Sharma, M. M. *Heterogeneous Reactions: Analysis, Examples, and Reactor Design.* U.SA: John Wiley & Sons, 1984.

[7] Balasubramania, S. N., Rihani, D. N. and Doraiswamy, L. K. " Film Model for Ethylene Dichloride Formation." *I&EC Fundamentals*, 5, No. 2 (1966), 184-188.

[8] Wachi, S. and Yousuke, A. "Kinetics of 1,2-dichloroethane Formation from Ethylene and Cupric Chloride." *I&EC Research*, 33 (1994), 259-264.

[9] Wachi, S. and Morikawa, H. " Chlorination of Ethylene in a Boiling Bubble Cloumn Reactor." *J. of Chem. Eng. of Japan*, 20, No. 3 (1987), 238-245.

[10] Miyauchi, T. and Vermeulen, T. " Diffusion and Back-flow Models for Two-Phase Axial Dispersion." *I&EC Fundamentals*, 2, No. 4 (1963), 304-309.

[11] Deckwer, W. D. and Hallensleben, J. " Exclusion of Gas Sparger Influence on Mass Transfer in Bubble Columns." *The Canadian J. of Chem. Eng*., 58 (1980), 190-197.

[12] Yeramian, A. A., Gottifredi , J. C. and Ronco, J. J. "Mass Transfer with Homogeneous Second Order Irreversible Reaction: A Note on An Explicit Expression for the Reaction Factor." *Chem. Eng. Sci*., 25 (1970), 1622-1625.

[13] Ueyama, K. and Miyauchi, T. "Properties of Recirculating Turbulent Two Phase Flow in Gas Bubble Columns." *AIChE J*, 25, No. 2 (1979), 258-266.

[14] Reklaitis, G. V. and Schneider, D. R. *Introduction to Material and Energy Balances.* USA: John Wiley & Sons, 1983.

إنتاج الإيثيلين ثنائي الكلور في المفاعلات ذات حلقة الدوران الخارجية

محمد البشير الأمين أبشر

قسم الهندسة الكيميائية ،كلية الهندسة، جامعة الملك سعود ،ص . ب. ٨٠٠،

الرياض ١١٤٢١، المملكة العربية السعودية

(قدم للنشر في ٢٠٠٢/٦/١٢م ؛ وقبل للنشر في ٢٠٠٢/١٠/٢٩م)

ملخص البحث. يشتمل البحث علي دراسة عملية ومحاكة نظرية لإنتاج الإيثيلين ثنائي الكلور من غاز الإيثيلين بواسطة الكلورة عند درجة الغليان في مفاعل ذي حلقة دوران خارجية. وجد أن هنالك تحسن ملحوظ لسلوك المفاعل عندما يستخدم موزّع الغاز ذي القرص المخرم أكثر من الموزع ذي الفوهة. ولقد تم أيضا اختبار صحة نموذج الخلايا الرياضي بواسطة المعلومات المعملية، ووجد أن النتائج من النموذج الرياضي تطابق النتائج المعملية. أستخدم النموذج الرياضي لدراسة تأثير بعض العوامل التصميمية والعملية علي سلوك المفاعل. وأوضحت النتائج بأن الأنظمة الطويلة مع استخدام زيادة في غاز الإيثيلين يؤدي إلى تحسن في تحوّل غاز الكلور.